

1 **Optically stimulated luminescence dating of heat retainer hearths from the Sahara: Insights**
2 **into signal accumulation and measurement.**

3
4 S.J. Armitage^{1,2*}, A. Krishna¹, L.E. Parker^{1,3}, G.E. King⁴

5
6 ¹Centre for Quaternary Research, Department of Geography, Royal Holloway, University of
7 London, Egham, Surrey, TW20 0EX, United Kingdom.

8 ²SFF Centre for Early Sapiens Behaviour (SapienCE), University of Bergen, Post Box 7805, 5020,
9 Bergen, Norway.

10 ³Archaeological Research Services Ltd, Angel House, Portland Square, Bakewell, Derbyshire,
11 DE45 1HB, United Kingdom.

12 ⁴Universität Bern, Institut für Geologie, Baltzerstrasse 1+3, 3012 Bern, Switzerland.

13
14 **Abstract**

15 Heat retainer hearths are a prominent component of the Holocene archaeological record of a number
16 of drylands. Rocks within these hearths were fired in antiquity, emptying the optically stimulated
17 luminescence (OSL) source traps of mineral grains within the rock. Since partial bleaching and
18 mixing of grains within a lithified heat retainer is impossible, these rocks offer the opportunity to
19 test our understanding of OSL signal accumulation and measurement processes. First, we show that
20 OSL ages calculated using grains size fractions from 4-11 μm up to 180-210 μm are
21 indistinguishable for a single heat retainer, indicating that the environmental and instrumental dose
22 rate correction factors routinely used in luminescence dating are accurate. Second, we used single-
23 grain dose recovery and equivalent dose measurements to determine the overdispersion due to beta
24 microdosimetry. For the heat retainers measured in this study, overdispersion due to beta
25 microdosimetry ranges from 8.9 ± 1.8 to 20.3 ± 1.6 %. Third, we investigate the impact of
26 mechanical crushing on the measured equivalent dose from quartz, to test the potential of using this
27 technique to liberate dateable material from heat retainers which are not acid soluble. A small (<1
28 Gy) but significant increase in equivalent dose is observed in crushed zero-age samples, but the
29 equivalent doses of crushed and uncrushed Holocene quartzes are indistinguishable. We conclude
30 that crushing is a viable method for extracting dateable material from a heat retainer, but that some
31 knowledge of the dosimeter's mean grain size is required for calculation of an accurate
32 environmental dose rate.

33

* e-mail: simon.armitage@rhul.ac.uk

34 *Keywords:* optically stimulated luminescence; hearths; dose rate; microdosimetry; crushing.

35

36 **1. Introduction**

37 Heat retainer hearths are a prominent component of the Holocene archaeological record, and are
38 particularly prevalent in the Sahara and Arabian Peninsula, where they are frequently associated with
39 surface scatters which attest to the presence of ancient nomadic pastoralists. Rocks, which acted as
40 heat retainers while the hearth was in use, are heated to sufficiently high temperatures to completely
41 empty the OSL source traps. Consequently, mineral grains from within these heat retainer rocks are
42 dateable using optically stimulated luminescence (OSL) techniques, providing an estimate of the time
43 elapsed since last firing (Armitage and King, 2013; Rhodes et al., 2010; Rhodes et al., 2009). These
44 fired heat retainers are often the only dateable and unequivocally anthropogenic component of the
45 surface archaeological record. OSL dating of hearths is therefore potentially an important tool for
46 understanding the nature of the surface archaeological record in drylands. Furthermore, fired hearth
47 stones offer a number of advantages when studying the accumulation of the OSL signal. First, since
48 the heat retainers are fired in a lithified state, and since post-firing mixing of mineral grains within a
49 heat retainer is impossible, OSL dating of multiple grain-size fractions from a single rock allows the
50 accuracy of grain-size specific corrections to environmental and instrumental dose rates to be tested.
51 Second, since post-firing mixing of mineral grains is impossible, and since Armitage and King (2013,
52 their Figure 5) have demonstrated that sunlight does not deplete the OSL signal in the inner portion
53 of hearth rocks, sand sized quartz extracted from hearth rocks may be used to investigate single-grain
54 equivalent dose (D_e) overdispersion due to beta microdosimetry. In the present study we: 1) Conduct
55 paired single-grain dose recovery and D_e measurement experiments to investigate the degree of
56 overdispersion caused by beta microdosimetry; 2) Calculate ages for a range of grain-size fractions
57 extracted from a single heat retainer to test the internal consistency of the OSL method, and 3)
58 Investigate the possibility of extending the OSL dating technique to non-carbonate lithologies where
59 mineral grains cannot be extracted from a heat retainer by acid dissolution.

60

61 **2 Materials and methods**

62 A total of thirteen heat retainers were collected from five hearths at the Al Wafa archaeological site,
63 in the Libyan Sahara. A full site description is found in Armitage and King (2013). Briefly, Al Wafa
64 is a gently sloping basin characterised by shallow, ephemeral drainage channels cut into an
65 extensively deflated surface composed of unconsolidated sand protected by gravel-pebble sized
66 carbonate clasts. The landscape is dominated by ~100 discrete hearths, which are usually seen as
67 mounds rising a few tens of centimetres above the surrounding land surface (Figure 1), and date from
68 ~7-9 ka (Armitage and King, 2013). These mounds are believed to result from topographic inversion,

69 with the hearths originally consisting of cobble lined pits dug into soil, which was subsequently
70 deflated when the Sahara dried ~5 ka (Armitage et al., 2015). The cobbles, which served as heat
71 retainers when the hearth was in use, are clasts of sandy limestone, which outcrops at the margin of
72 the Al Wafa basin. Approximately cuboid heat retainers with no visible fracturing were sampled from
73 discrete hearths.

74
75 The outer light exposed portions of the heat retainers was removed by repeated immersion in 1.16 M
76 HCl, until the length of each axis of the clast had been reduced by a minimum of 25 mm. The dating
77 sample was obtained by dissolution of the remaining material. Quartz separates were produced using
78 the methods summarised in Supplemental Material Section A. For samples FZ39-48, only the 210-
79 180 μm fraction was prepared for measurement. For samples FZ84, 85, 95 and 96, dating samples
80 were prepared from the 4-11, 11-20, 20-40, 40-60, 60-90, 90-125, 125-150, 150-180 and 180-210 μm
81 fractions. All size fractions were mounted on 10 mm aluminium discs. Additional single-grain
82 analysis (212-180 μm grains) was performed using standard Risø single-grain sample holders.

83
84 All OSL measurements presented in this study were carried out using a Risø TL/OSL-DA-15 dating
85 system (Bøtter-Jensen et al., 2003), fitted with a single-grain OSL attachment (Duller et al., 1999).
86 Optical stimulation of single aliquots was carried out using a blue (470 ± 30 nm) light emitting diode
87 (LED) array with a power density of 33 mW/cm^2 , while single-grains were stimulated using a 10 mW
88 Nd : YVO₄ solid-state diode-pumped green laser (532 nm) focussed to yield a nominal power density
89 of 50 W/cm^2 . Infra-red (IR) stimulation was carried out using an IR (870 nm) laser diode array. OSL
90 was measured using an Electron Tubes Ltd 9235QB15 photomultiplier tube with 7.5 mm of Hoya U-
91 340 filter interposed between the sample and photomultiplier. Irradiation was carried out using a 40
92 mCi ⁹⁰Sr/⁹⁰Y beta source, calibrated relative to the National Physical Laboratory, Teddington ⁶⁰Co γ -
93 source (Hotspot 800) (Armitage and Bailey, 2005b). Due to the spatial heterogeneity of beta emitters
94 across the active face of the ⁹⁰Sr/⁹⁰Y beta source, it was necessary to apply a grain position correction
95 to single-grain D_e values, using the method of (Armitage et al., 2011).

96
97 Equivalent doses were determined using the single-aliquot regenerative-dose (SAR) method (Murray
98 and Wintle, 2000). Following Armitage and King (2013), who worked on heat retainers from the Al
99 Wafa site, we adopted a preheating regime of 260 °C, 10 s for PH1 (the pre-heat prior to measurement
100 of natural or regenerated luminescence) and 220 °C, 10 s for PH2 (the pre-heat prior to measurement
101 of the test dose luminescence response) for all measurements. OSL measurements were made at 125
102 °C, using blue diodes (40 s) for aliquot measurements or a green laser (2 s per grain) for single-grain
103 measurements. For blue diode stimulation, the OSL signal was that recorded during the first 0.36 s of

104 stimulation, and a background signal from the last 4 s of stimulation was subtracted. For green laser
105 stimulation, the OSL signal was that recorded during the first 0.3 s of stimulation, and a background
106 signal from the last 0.3 s of stimulation was subtracted (Thomsen et al., 2005). Curve fitting, and D_e
107 determination, were performed using version 3.24 of the Luminescence Analyst software (Duller,
108 2007). We adopted the single-grain rejection criteria of Armitage et al. (2011), Supplementary
109 Material Section B.

110

111 **3 Age estimates generated using different grain-size fractions**

112 In principle, any grain-size fraction from fine silt to fine sand can be used to measure the equivalent
113 dose of a sample. For any given sample, the grain size used may be dictated by availability or the
114 post-depositional processes which a sample has experienced e.g. silt may be translocated by
115 percolating water in a sandy sediment, but be the only clast size available in a loess deposit.
116 Consequently, sedimentary characteristics and geomorphic setting often necessitates the
117 measurement of different grain size fractions for samples within the same dating study. However,
118 numerous factors determining the environmental or laboratory dose rate experienced by the
119 luminescence dosimeter vary with grain size. These variations may be progressive, e.g. the ~13%
120 increase in beta dose rate from a Risø irradiation unit as grain size increases from 4-11 μm to $>63 \mu\text{m}$
121 (Armitage and Bailey, 2005b) or abrupt e.g. at the transition between sand-sized material, which are
122 routinely etched to remove the alpha dosed rind, and silt-sized material. If a single dating project uses
123 more than one grain size fraction, then the minimum requirement for a successful study is that
124 different grain sizes yield the same luminescence age for sediments which were deposited
125 simultaneously. In practice, the types of sedimentary deposit which are normally targeted for OSL
126 dating tend to be well sorted. Conversely, the heat retainers from Al Wafa contain quartz grains from
127 <4 to $>210 \mu\text{m}$ in diameter, all of which must have a common OSL age, making these samples ideal
128 for testing the internal consistency of OSL ages produced using different grain size fractions.

129

130 Twelve aliquots of quartz from each size fraction from each of four samples were measured using a
131 single luminescence reader. Across the range of grain sizes measured, progressive variations in
132 environmental alpha (Brennan et al., 1991) and beta (Guérin and Mercier, 2012) attenuation factors,
133 and laboratory beta dose rate (Armitage and Bailey, 2005b) occurred. An abrupt alteration in dose
134 rate occurred between the 60-90 and 90-125 μm fractions due to HF etching of $>90 \mu\text{m}$ grains,
135 resulting in the loss of 100% of the environmental alpha dose (making the common assumption of
136 isotropic etching), and 1% of the environmental beta dose (Brennan, 2003). An abrupt change in
137 laboratory dose rate is also present between 20-40 and 40-60 μm , since the $<40 \mu\text{m}$ grains were
138 deposited from suspension, coating the entire face of the disc, whereas the $>40 \mu\text{m}$ grains were

139 attached using Silkospray applied via a 5 mm diameter mask. However, since the instrument was
140 calibrated using samples mounted by the same methods, no correction for the known variation in
141 instrumental dose rate between the core and periphery of the disc was made (Ballarini et al., 2006).

142
143 Equivalent dose, dose rate and calculated age are presented for nine different grain size fractions in
144 the range 4-210 μm (Tables S2-S4). For sample FZ84 (Figure 2), dose rate falls steadily as grain size
145 increases, from a value of 0.98 ± 0.07 Gy/ka (4-11 μm) to 0.83 ± 0.05 Gy/ka (180-212 μm), a decrease
146 of ~18 %. For all four of the samples for which data are available, equivalent dose also falls with
147 increasing grain size, though for each sample there are outliers from this general trend (e.g. 11-20 μm
148 in Figure 2). Nonetheless, ages calculated for each grain size fraction from a single sample are
149 consistent with each other. This result indicates that for these samples at least, the dose rate correction
150 factors used in this study produce consistent ages across the full range of grain sizes commonly
151 adopted for luminescence dating work.

152

153 **4 Single-grain overdispersion due to beta microdosimetry**

154 Overdispersion (OD), the relative spread of equivalent doses after measurement uncertainties are
155 excluded, is a key input for several of the statistical models used in single-grain dating e.g. the
156 Minimum Age Model (MAM) (Galbraith et al., 1999) and the Finite Mixture Model (FMM) .
157 However, successful application of these models requires an estimate of the OD of a well-bleached
158 sample, which is otherwise identical to the sample being measured. Incorrect estimation of the well-
159 bleached OD may lead to the adoption of the incorrect statistical model, and the production of an
160 incorrect age. For example, an erroneously young age would be calculated if an underestimate of the
161 well-bleached OD caused the MAM to be applied to a sample that was not partially bleached. The
162 heterogeneous distribution of beta activity within a sediment, e.g. where occasional potassium
163 feldspars are present within a quartz rich sand (Mayya et al., 2006), has the potential to cause such an
164 underestimation of the well-bleached OD. Although some success has been achieved in modelling
165 OD due to beta microdosimetry (Cunningham et al., 2012; Guérin et al., 2015; Martin et al., 2015),
166 few studies have measured OD in ancient sediments where other causes may be excluded or isolated.
167 Heat retainers which were fired in antiquity offer the opportunity to isolate OD due to beta
168 microdosimetry, since lithified samples cannot experience post-depositional mixing, and firing
169 completely empties the OSL source traps (Armitage and King, 2013, section 8), eliminating the
170 possibility of heterogeneous bleaching. Consequently, OD observed in a D_e dataset (OD_{D_e}) from a
171 heat retainer consists of contributions from the measurement process (e.g. instrumental variability
172 and intra-sample variation in luminescence characteristics) and from beta microdosimetry. Since the
173 OD observed in a dose recovery dataset (OD_{Rec}) is caused by the measurement process alone, it is

174 possible to isolate OD due to beta microdosimetry (OD_{β}) by subtracting quadratically OD_{Rec} from
175 OD_{De} .

176

177 Dose recovery measurements were made on six samples from Al Wafa. Following Armitage and
178 King (2013), single-grain dose recovery experiments were performed by heating samples to 350 °C
179 for 120 s (to empty the OSL source traps) after which a beta dose similar to D_e (the “known dose”)
180 was applied. The “recovered dose” was then measured, using an identical measurement sequence to
181 that used for measuring the equivalent dose. Single-grain equivalent dose, dose recovery and OD
182 values are presented in Table S6. The “dose recovery ratios” (recovered dose/known dose) ranged
183 from 0.96 ± 0.01 to 1.00 ± 0.01 , with a mean value of 0.99 ± 0.01 , indicating that the measurement
184 parameters used in this study are appropriate for the Al Wafa samples. OD_{rec} values ranged from 6.3
185 $\pm 0.6 \%$ to $9.7 \pm 1.1 \%$, with a mean value of $7.6 \pm 1.2 \%$. OD_{β} values ranged from 15.8 ± 1.8 to
186 $27.1 \pm 1.6 \%$, with a mean value of 22.6 ± 4.1 , while OD_{De} values ranged from $18.5 \pm 1.5 \%$ to 28.2
187 $\pm 1.5 \%$, with a mean value of $23.9 \pm 3.6 \%$.

188

189 The wide range of OD_{β} values from heat retainers from a single location, and derived from a single
190 geological unit, suggests that the effects of beta microdosimetry is highly sample dependant. This
191 implies that, even for multiple samples from a single location, the well-bleached OD required for the
192 application of several statistical models may need to be determined for each individual sample. In
193 addition, only one of the six samples measured yielded an OD_{De} value below 20%. Several studies
194 (e.g. Armitage et al., 2011) have used an OD_{De} value of 20% to distinguish between well-bleached,
195 undisturbed samples ($OD_{De} < 20\%$) and samples which have been subject to partial bleaching or post
196 depositional mixing ($OD_{De} > 20\%$). Our results contribute to a growing body of literature (Guérin et
197 al., 2015; Thomsen et al., 2016) which does not support the use of a 20% OD_{De} threshold. Instead a
198 site-specific, or possibly even a sample specific, OD_{De} estimate for a well-bleached sample is
199 required. In the absence of such an estimate, partial bleaching or post depositional mixing should be
200 diagnosed based upon a knowledge of the sample’s depositional context and burial history. This
201 approach risks confirmation bias (the tendency to observe effects which are expected to be present),
202 and highlights the need for a robust method for estimating the OD expected from a well-bleached
203 sample.

204

205 **5 Extending the OSL dating technique to non-carbonate lithologies**

206 Where heat retainers are composed of carbonate rock, extraction of dateable material is easily
207 achieved using progressive HCl dissolution to remove the outer light-exposed portions of the rock
208 (e.g. Armitage and King, 2013). Conversely non-carbonate heat retainers have been subject to more

209 complicated preparation procedures. For example, Rhodes et al. (2010) removed the light exposed
210 portion of the rock using a geological hammer, followed by two cycles of mechanical crushing (one
211 producing pebble sized fragments, and the other yielding sand sized fragments) and a short HF etch
212 to remove surface crushing effects and feldspar. This latter approach has the disadvantage of being
213 time-consuming and, depending upon the mineralogical composition of the parent rock, potentially
214 yielding a polymineral sample with unpredictable luminescence characteristics. An alternative
215 approach is to remove the outer portions of the rock with a geological hammer, and crush the
216 remaining dating fraction in a mill, preparing the resulting powder using the standard method for 4-
217 11 μm silt. The advantages of this approach is that it is less labour intensive, is likely to yield a more
218 predictably pure quartz separate, and presents the sample to the luminescence reader in a predictable
219 geometry. As with the method of Rhodes et al, (2010), this method requires a realistic approximation
220 of the mean grain size of the dosimeter before crushing to calculate an accurate dose rate. More
221 significantly, a crushing induced increase in signal has been observed for burnt flint samples (Aitken,
222 1985), section 7.1), while recent evidence suggests that crushing or shearing may either reduce or
223 reset the natural luminescence signal (Bateman et al., 2012; Swift et al., 2011).

224

225 To test the possibility that milling induces a luminescence signal, a selection of seven zero age quartz
226 separates were measured in their crushed and uncrushed states. Similarly, to test the possibility that
227 milling reduces the luminescence signal, a selection of five quartz separates from Holocene dune
228 samples (D_e ranging from 2-20 Gy) were measured in their crushed and uncrushed states. Finally, to
229 test the utility of crushing as a method for extracting dateable quartz from non-carbonate heat
230 retainers, small chips from the core of the four heat retainers reported in Section 3 were crushed, and
231 the D_e compared to that for material extracted via sequential dissolution in HCl. Crushed samples
232 were prepared by loading ~ 2 g of material into a light-tight stainless steel grinding jar, and grinding
233 at 20 Hz for 120 s using a Retsch Mixer Mill MM400. The 4-11 μm fraction was subsequently
234 extracted from the milled material using the method described in Supplemental Material Section A.
235 Results are presented in Supplementary Material Tables 3-5.

236

237 Of the seven zero age samples measured (Table S7), four showed a significant increase in equivalent
238 dose upon crushing, while three yielded indistinguishable values. The mean increase in equivalent
239 dose due to crushing was 0.25 ± 0.14 Gy, ranging from 0.08 ± 0.05 Gy for a Libyan desert dune sand
240 (Armitage et al., 2007) to 0.93 ± 0.33 Gy for a South African coastal dune sand (this study). From
241 these data it is apparent that crushing can induce a significant increase in D_e , but that the effect is
242 neither universal nor uniform. None of the five Holocene samples yielded crushed/uncrushed ratios
243 distinguishable from unity (Table S8), suggesting that any signal increase due to crushing is either

244 negligible or masked by other sources of D_e scatter. Crushed material from the cores of the four heat
245 retainers yielded equivalent doses consistent with the range of values obtained from uncrushed
246 material (Tables S2-S5). However, to determine an age, the mean grain size of the uncrushed quartz
247 must be known to determine the applicable dose rate. Without this information i.e. assuming mean
248 grain size of the dosimeter to be somewhere between 4 and 210 μm , a large uncertainty term needs
249 to be used to account for the $\sim 15\%$ variation in environmental dose rate between these grain sizes.
250 In the case of the four heat retainers measured here, the effective grain size of the quartz prior to
251 crushing may be determined by calculating the dose rate required for the equivalent dose of the
252 crushed material to yield the mean age determined using the various grain size fractions presented in
253 Section 3. This analysis indicates that heat retainers contained grains with a mean effective size of
254 40-60 μm (n=2), 90-150 μm (n=1) and >210 μm (n=1). For the samples in question, environmental
255 dose rates decrease by $7.7 \pm 0.8\%$ from 40-60 to 180-210 μm . Consequently, estimation of the mean
256 grain size either by visual inspection or petrography may yield acceptably precise estimates of the
257 environmental dose rate. These data suggest that crushing is a viable technique for extracting dateable
258 mineral separates from heat retainers with non-carbonate lithologies.

259

260 **6 Conclusions**

261 Heat retainers from ancient hearths offer the opportunity to test our understanding of OSL signal
262 accumulation and measurement processes. We measure equivalent doses from a range of grain sizes
263 commonly adopted in luminescence dating studies. For each hearth stone, different size fractions
264 yield similar ages, indicating that for our samples at least, the instrumental and environmental dose
265 rate correction factors used in luminescence dating yield internally consistent (accurate?) results. In
266 addition, since mineral grains within heat retainers cannot be subject to partial bleaching or post firing
267 mixing, overdispersion in single-grain data from these samples is due to measurement processes and
268 beta microdosimetry. The latter may be isolated by subtracting quadratically the single-grain
269 overdispersion obtained from a dose recovery experiment on the same sample. This approach yielded
270 values for overdispersion resulting from beta microdosimetry ranging from 15.8 ± 1.8 to 27.1 ± 1.6
271 %. Our results suggest that the application of a standard overdispersion threshold (e.g. 20%), above
272 which processes such as mixing or partial bleaching may be diagnosed, may not yield accurate results.
273 Lastly, the possibility of extracting dateable material from heat retainers via mechanical crushing was
274 explored. A small but significant increase in equivalent dose was observed for a number of quartz
275 separates from zero-age samples after crushing. However, it was not possible to distinguish the
276 equivalent dose from crushed and uncrushed fractions of five Holocene samples. These results
277 suggest that crushing is a viable method for extracting dateable material from a rock, but we note that

278 some knowledge of the dosimeter's mean grain size is required for calculation of an accurate
279 environmental dose rate.

280

281 **7 Acknowledgements**

282 SJA's contribution to this work was partly supported by the Research Council of Norway, through its
283 Centres of Excellence funding scheme, SFF Centre for Early Sapiens Behaviour (SapienCE), project
284 number 262618. GEK acknowledges support from Swiss National Science Foundation grant number
285 PZ00P2-167960.

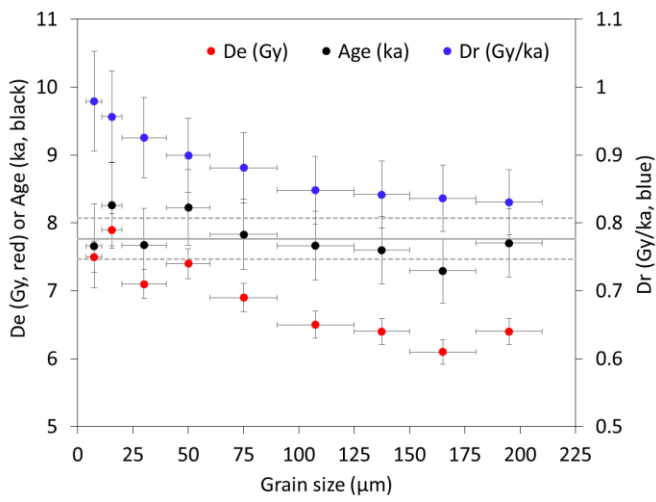
286 **Figures**



287

288 Figure 1: A small hearth at Al Wafa. The hearth mound is ~1 m in diameter.

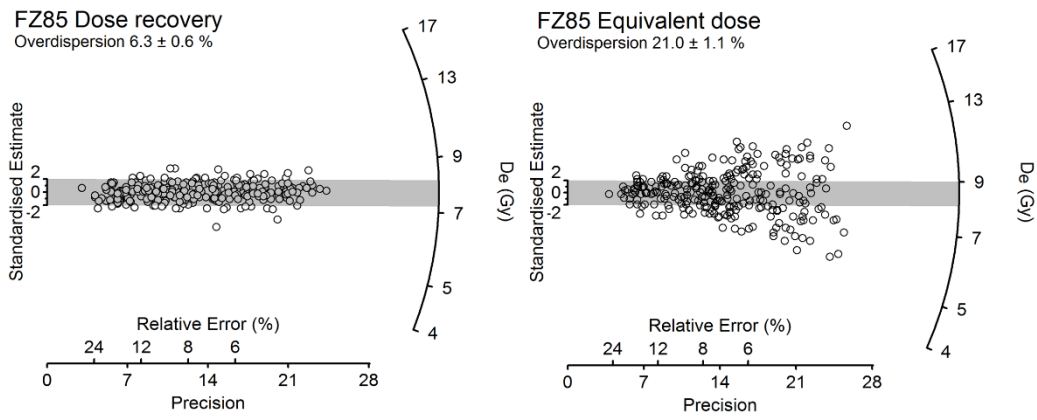
289



290

291 Figure 2: Equivalent dose (D_e), environmental dose rate (D_r) and calculated age for different grain
 292 size fractions of quartz from heat retainer sample FZ84. The thick grey line represents the mean
 293 age, calculated using data from all grain sizes, while the dashed lines represent ± 1 standard
 294 deviation.

295



296

297 Figure 3: Radial plots of equivalent doses for individual quartz grains from heat retainer sample
 298 FZ85. The grey bars are centred at the equivalent dose calculated using the central age model
 299 (Galbraith et al., 1999). The left radial plot represents data from a dose recovery experiment,
 300 whereas the right panel shows the natural equivalent dose distribution.

301

302

303

304
305
306
307
308
309
310
311
312
313
314
315
316
317
318
319
320
321
322
323
324
325
326
327
328
329
330
331
332
333
334
335
336
337
338
339
340
341
342
343
344
345
346
347
348
349
350
351
352
353

References

Aitken, M.J., 1985. Thermoluminescence dating. Academic press.

Armitage, S.J., Bailey, R.M., 2005. The measured dependence of laboratory beta dose rates on sample grain size. *Radiat Meas* 39, 123-127.

Armitage, S.J., Bristow, C.S., Drake, N.A., 2015. West African monsoon dynamics inferred from abrupt fluctuations of Lake Mega-Chad. *P Natl Acad Sci USA* 112, 8543-8548.

Armitage, S.J., Drake, N.A., Stokes, S., El-Hawat, A., Salem, M., White, K., Turner, P., McLaren, S.J., 2007. Multiple phases of north African humidity recorded in lacustrine sediments from the fazzan basin, Libyan sahara. *Quat Geochronol* 2, 181-186.

Armitage, S.J., Jasim, S.A., Marks, A.E., Parker, A.G., Usik, V.I., Uerpmann, H.-P., 2011. The Southern Route "Out of Africa": Evidence for an Early Expansion of Modern Humans into Arabia. *Science* 331, 453-456.

Armitage, S.J., King, G.E., 2013. Optically stimulated luminescence dating of hearths from the Fazzan Basin, Libya: A tool for determining the timing and pattern of Holocene occupation of the Sahara. *Quat Geochronol* 15, 88-97.

Ballarini, M., Wintle, A.G., Wallinga, J., 2006. Spatial variation of dose rate from beta sources as measured using single grains. *Ancient TL* 24, 1-7.

Bateman, M.D., Swift, D.A., Piotrowski, J.A., Sanderson, D.C.W., 2012. Investigating the effects of glacial shearing of sediment on luminescence. *Quat Geochronol* 10, 230-236.

Bøtter-Jensen, L., Andersen, C.E., Duller, G.A.T., Murray, A.S., 2003. Developments in radiation, stimulation and observation facilities in luminescence measurements. *Radiat Meas* 37, 535-541.

Brennan, B.J., 2003. Beta doses to spherical grains. *Radiat Meas* 37, 299-303.

Brennan, B.J., Lyons, R.G., Phillips, S.W., 1991. Attenuation of alpha particle track dose for spherical grains. *International Journal of Radiation Applications and Instrumentation. Part 18*, 249-253.

Cunningham, A.C., Devries, D.J., Schaart, D.R., 2012. Experimental and computational simulation of beta-dose heterogeneity in sediment. *Radiat Meas* 47, 1060-1067.

Duller, G., 2007. Assessing the error on equivalent dose estimates derived from single aliquot regenerative dose measurements. *Ancient TL* 25, 15-24.

Duller, G.A.T., Bøtter-Jensen, L., Murray, A.S., Truscott, A.J., 1999. Single grain laser luminescence (SGLL) measurements using a novel automated reader. *Nuclear Instruments and Methods in Physics Research, Section B: Beam Interactions with Materials and Atoms* 155, 506-514.

Galbraith, R.F., Roberts, R.G., Laslett, G.M., Yoshida, H., Olley, J.M., 1999. Optical dating of single and multiple grains of quartz from Jinmium rock shelter, northern Australia: Part I, experimental design and statistical models. *Archaeometry* 41, 339-364.

Guérin, G., Jain, M., J. Thomsen, K., S. Murray, A., Mercier, N., 2015. Modelling dose rate to single grains of quartz in well-sorted sand samples: The dispersion arising from the presence of potassium feldspars and implications for single grain OSL dating. *Quat Geochronol* 27, 52-65.

Guérin, G., Mercier, N., 2012. Preliminary insight into dose deposition processes in sedimentary media on a scale of single grains: Monte Carlo modelling of the effect of water on the gamma dose rate. *Radiat Meas* 47, 541-547.

Martin, L., Mercier, N., Incerti, S., Lefrais, Y., Pecheyran, C., Guérin, G., Jarry, M., Bruxelles, L., Bon, F., Pallier, C., 2015. Dosimetric study of sediments at the beta dose rate scale: Characterization and modelization with the DosiVox software. *Radiat Meas* 81, 134-141.

Mayya, Y.S., Morthekai, P., Murari, M.K., Singhvi, A.K., 2006. Towards quantifying beta microdosimetric effects in single-grain quartz dose distribution. *Radiat Meas* 41, 1032-1039.

Murray, A.S., Wintle, A.G., 2000. Luminescence dating of quartz using an improved single-aliquot regenerative-dose protocol. *Radiat Meas* 32, 57-73.

354 Rhodes, E.J., Fanning, P.C., Holdaway, S.J., 2010. Developments in optically stimulated
355 luminescence age control for geoarchaeological sediments and hearths in western New South
356 Wales, Australia. *Quat Geochronol* 5, 348-352.

357 Rhodes, E.J., Fanning, P.C., Holdaway, S.J., Bolton, C.C., 2009. Archaeological surfaces in western
358 NSW: stratigraphic contexts and preliminary OSL dating of hearths. *Terra Australis* 28, 12.

359 Swift, D.A., Sanderson, D.C.W., Nienow, P.W., Bingham, R.G., Cochrane, I.C., 2011. Anomalous
360 luminescence of subglacial sediment at Haut Glacier d'Arolla, Switzerland - a consequence of
361 resetting at the glacier bed? *Boreas* 40, 446-458.

362 Thomsen, K.J., Murray, A.S., Bøtter-Jensen, L., 2005. Sources of variability in OSL dose
363 measurements using single grains of quartz. *Radiat Meas* 39, 47-61.

364 Thomsen, K.J., Murray, A.S., Buylaert, J.P., Jain, M., Hansen, J.H., Aubry, T., 2016. Testing
365 single-grain quartz OSL methods using sediment samples with independent age control from the
366 Bordes-Fitte rockshelter (Roches d'Abilly site, Central France). *Quat Geochronol* 31, 77-96.

367
368

369 **Supplementary material for “Optically stimulated luminescence dating of heat retainer**
370 **hearthths from the Sahara: Insights into signal accumulation and measurement.” Armitage et**
371 **al.**

372
373 **A. Sample preparation procedure**

374 Having removed the light exposed layers of the heat retainer, dating samples were prepared using
375 standard laboratory techniques. Briefly, carbonate was removed by immersion in 1.16 M HCl,
376 followed by immersion in H₂O₂ to oxidise organic material. Samples FZ84, 85, 95 and 96 were sieved
377 at 40 µm, and the material which passed through the mesh was subsequently Stokes settled to 4-11,
378 11-20 and 20-40 µm. Material retained in the mesh was sieved to yield 40-60, 60-90, 90-125, 125-
379 150, 150-180 and 180-210 size fractions. Quartz was extracted from the <90 µm fractions via
380 prolonged immersion in H₂SiF₆. Quartz was extracted from the >90 µm fractions via density
381 separation at 2.62 and 2.75 g/cm³, and 1 hour immersion in 23 M HF. Following H₂SiF₆ or HF
382 treatment, samples were immersed 11 M HCl for a minimum of 12 hours to remove fluoride
383 precipitates. The <60 µm fractions were settled from suspension onto 10 mm diameter aluminium
384 discs, resulting in a monolayer of quartz across the entire upper face of the disc. The >60 µm fractions
385 were mounted on aluminium discs using Silkospray silicone oil applied via a 5 mm mask, resulting
386 in a monolayer of grains across the middle 5 mm of the disc. Single-grain analysis was performed on
387 180-210 µm grains mounted in Risø single-grain sample holders, containing a 10x10 array of 300 µm
388 diameter holes. Sample preparation and mounting methods are summarised in Table S1.
389

390 Table S1. Summary sample preparation and mounting methods for the various grain size fractions reported in this study.

Grain size (µm)	Size separation method	Quartz purification method	Sample mounting method
4-11			
11-20	Stokes settling		Settled from suspension
20-40		H ₂ SiF ₆ + HCl	
40-60			
60-90			
90-125	Sieve		Silkospray silicone oil via a 5 mm mask
125-150		Density separation + HF	
150-180			
180-210			

391

392 **B. Single-grain rejection criteria.**

393 Grains were rejected where one or more of the following conditions are met: (1) the T_n signal from
394 the grain is too low to distinguish it from the variability in the background signal (the difference
395 between T_n and the average count from the background interval is less than three times the standard
396 deviation of the counts in the background interval, determined using the “sig. >3 sigma above BG”
397 rejection criterion in Luminescence Analyst, (Duller, 2007)); (2) the recycling ratio (Murray and
398 Wintle, 2000) differs from unity by greater than 10%; (3) the OSL IR-depletion ratio (Duller, 2003)
399 is greater than two standard errors below unity; (4) recuperation is high (i.e. L_x/T_x for the 0 Gy
400 regeneration point is greater than 5% of L_n/T_n, (Murray and Wintle, 2000)); (5) L_n/T_n does not
401 intercept the growth curve (Armitage et al., 2000; Bailey et al., 2005) – no grains failed this criterion
402 due to the low D_e of the samples, or (6) the dose response curve shape precludes the generation of a
403 meaningful equivalent dose. Unlike the other five criteria, criterion six requires user-judgement and
404 hence cannot be applied mechanistically. It was used where the signal does not increase
405 monotonically in response to increasing dose, or where L_n/T_n intercepted the dose-response curve at
406 the point where growth ceased, with the former being more common.
407

407

408

409 **C. Equivalent dose, dose rate and calculated age for different size fractions from Al Wafa heat**
 410 **retainers.**

411 Equivalent dose (D_e), dose rate and calculated age data for different size fractions from Al Wafa heat
 412 retainers are presented in Tables S2-S5. In these tables, “Mean 4-210” denotes the mean age
 413 determined for grain size fraction in the range 4-210 μm . The “effective grain size” is calculated as
 414 the grain size with a dose rate which yields the mean 4-210 μm age for the 4-11 μm quartz produced
 415 by crushing the bulk sample (Section 5). Dose rates and ages are calculated using a mean water
 416 content of $5\pm 2\%$, a burial depth of 30 cm (yielding a cosmic dose rate of 0.235 ± 0.020 Gy/ka) and
 417 partitioning the gamma dose between the heat retainer and underlying sediments (Armitage and King,
 418 2013). For alpha dose rates, an a-value of 0.04 ± 0.02 was used throughout. Instrumental beta dose
 419 rates were corrected for grain size using the values measured by Armitage and Bailey (2005, Table
 420 1).

421
 422 Table S2: Heat retainer FZ84

Grain size (μm)	D_e (Gy)	Dose rates (Gy/ka)				Age (ka)
		Alpha	Beta	Gamma	Total	
4-11	7.5 ± 0.2	0.10 ± 0.05	0.41 ± 0.04	0.23 ± 0.02	0.98 ± 0.07	7.7 ± 0.6
11-20	7.9 ± 0.2	0.08 ± 0.04	0.41 ± 0.04	0.23 ± 0.02	0.96 ± 0.07	8.3 ± 0.6
20-40	7.1 ± 0.2	0.06 ± 0.03	0.40 ± 0.04	0.23 ± 0.02	0.93 ± 0.06	7.7 ± 0.5
40-60	7.4 ± 0.2	0.04 ± 0.02	0.40 ± 0.04	0.23 ± 0.02	0.90 ± 0.05	8.2 ± 0.6
60-90	6.9 ± 0.2	0.03 ± 0.01	0.39 ± 0.04	0.23 ± 0.02	0.88 ± 0.05	7.8 ± 0.5
90-125	6.5 ± 0.2	-	0.39 ± 0.04	0.23 ± 0.02	0.85 ± 0.05	7.7 ± 0.5
125-150	6.4 ± 0.2	-	0.38 ± 0.04	0.23 ± 0.02	0.84 ± 0.05	7.6 ± 0.5
150-180	6.1 ± 0.2	-	0.37 ± 0.04	0.23 ± 0.02	0.84 ± 0.05	7.3 ± 0.5
180-210	6.4 ± 0.2	-	0.37 ± 0.04	0.23 ± 0.02	0.83 ± 0.05	7.7 ± 0.5
Mean 4-210	-	-	-	-	-	7.8 ± 0.5
Effective grain size 40-60 μm						
4-11 (crushed)	7.0 ± 0.2				0.90 ± 0.05	7.8 ± 0.5

423
 424 Table S3: Heat retainer FZ85

Grain size (μm)	D_e (Gy)	Dose rates (Gy/ka)				Age (ka)
		Alpha	Beta	Gamma	Total	
4-11	10.7 ± 0.3	0.10 ± 0.05	0.37 ± 0.04	0.22 ± 0.02	0.93 ± 0.07	11.5 ± 0.9
11-20	10.8 ± 0.3	0.09 ± 0.04	0.36 ± 0.04	0.22 ± 0.02	0.91 ± 0.07	11.9 ± 0.9
20-40	10.1 ± 0.3	0.06 ± 0.03	0.36 ± 0.04	0.22 ± 0.02	0.88 ± 0.06	11.5 ± 0.8
40-60	9.6 ± 0.3	0.04 ± 0.02	0.35 ± 0.04	0.22 ± 0.02	0.85 ± 0.05	11.3 ± 0.8
60-90	9.4 ± 0.3	0.03 ± 0.01	0.35 ± 0.04	0.22 ± 0.02	0.84 ± 0.05	11.3 ± 0.7
90-125	8.6 ± 0.3	-	0.34 ± 0.04	0.22 ± 0.02	0.80 ± 0.05	10.7 ± 0.7
125-150	8.6 ± 0.3	-	0.34 ± 0.04	0.22 ± 0.02	0.80 ± 0.05	10.8 ± 0.7
150-180	8.3 ± 0.3	-	0.33 ± 0.04	0.22 ± 0.02	0.79 ± 0.05	10.5 ± 0.7
180-210	8.9 ± 0.3	-	0.33 ± 0.04	0.22 ± 0.02	0.79 ± 0.04	11.3 ± 0.7
Mean 4-210	-	-	-	-	-	11.2 ± 0.8
Effective grain size 40-60 μm						
4-11 (crushed)	9.5 ± 0.3				0.85 ± 0.05	11.2 ± 0.8

425
 426
 427

Table S4: Heat retainer FZ95

Grain size (μm)	D_e (Gy)	Dose rates (Gy/ka)				Age (ka)
		Alpha	Beta	Gamma	Total	
4-11	5.8 ± 0.2	0.07 ± 0.04	0.32 ± 0.03	0.22 ± 0.02	0.85 ± 0.06	6.9 ± 0.5
11-20	9.4 ± 0.3	0.06 ± 0.03	0.32 ± 0.03	0.22 ± 0.02	0.83 ± 0.05	$11.3 \pm 0.8^*$
20-40	4.1 ± 0.1	0.04 ± 0.02	0.31 ± 0.03	0.22 ± 0.02	0.81 ± 0.05	5.1 ± 0.3
40-60	4.8 ± 0.1	0.03 ± 0.01	0.31 ± 0.03	0.22 ± 0.02	0.79 ± 0.04	6.1 ± 0.4
60-90	4.8 ± 0.1	0.02 ± 0.01	0.31 ± 0.03	0.22 ± 0.02	0.77 ± 0.04	6.2 ± 0.4
90-125	4.3 ± 0.1	-	0.30 ± 0.03	0.22 ± 0.02	0.75 ± 0.04	5.7 ± 0.4
125-150	4.6 ± 0.1	-	0.29 ± 0.03	0.22 ± 0.02	0.75 ± 0.04	6.2 ± 0.4
150-180	6.2 ± 0.2	-	0.29 ± 0.03	0.22 ± 0.02	0.74 ± 0.04	8.4 ± 0.5
180-210	4.4 ± 0.1	-	0.29 ± 0.03	0.22 ± 0.02	0.74 ± 0.04	6.0 ± 0.4
Mean 4-210	-	-	-	-	-	6.3 ± 1.0
Effective grain size 90-150 μm						
4-11 (crushed)	4.7 ± 0.1				0.75 ± 0.04	6.3 ± 0.4

*The age for 11-20 μm grain size has been omitted from the calculation of the mean age.

429

430

431

Table S5: Heat retainer FZ96

Grain size (μm)	D_e (Gy)	Dose rates (Gy/ka)				Age (ka)
		Alpha	Beta	Gamma	Total	
4-11	7.9 ± 0.2	0.07 ± 0.04	0.53 ± 0.06	0.24 ± 0.02	1.09 ± 0.07	7.3 ± 0.5
11-20	8.4 ± 0.2	0.06 ± 0.03	0.53 ± 0.06	0.24 ± 0.02	1.07 ± 0.07	7.9 ± 0.6
20-40	7.4 ± 0.2	0.04 ± 0.02	0.52 ± 0.06	0.24 ± 0.02	1.04 ± 0.07	7.1 ± 0.5
40-60	6.9 ± 0.2	0.03 ± 0.02	0.51 ± 0.06	0.24 ± 0.02	1.02 ± 0.06	6.8 ± 0.5
60-90	6.3 ± 0.2	0.02 ± 0.01	0.51 ± 0.05	0.24 ± 0.02	1.00 ± 0.06	6.3 ± 0.4
90-125	6.7 ± 0.2	-	0.50 ± 0.05	0.24 ± 0.02	0.98 ± 0.06	6.9 ± 0.5
125-150	6.2 ± 0.2	-	0.49 ± 0.05	0.24 ± 0.02	0.97 ± 0.06	6.4 ± 0.4
150-180	5.9 ± 0.2	-	0.48 ± 0.05	0.24 ± 0.02	0.96 ± 0.06	6.1 ± 0.4
180-210	5.9 ± 0.2	-	0.47 ± 0.05	0.24 ± 0.02	0.95 ± 0.06	6.2 ± 0.4
Mean 4-210	-	-	-	-	-	6.8 ± 0.6
Effective grain size $>210 \mu\text{m}$						
4-11 (crushed)	5.9 ± 0.2				0.87 ± 0.06	6.8 ± 0.5

432

433

434

D. Single grain overdispersion values

435

436

Table S6: Single-grain equivalent dose, dose recovery and overdispersion data.

Sample	Equivalent dose data			Dose recovery data			OD_β (%)
	D_e (Gy)	Grains (accepted/measured)	OD_{D_e} (%)	Ratio (recovered/known)	Grains (accepted/measured)	OD_{Rec} (%)	
FZ40	9.2 ± 0.3	131/1000	18.5 ± 1.5	0.98 ± 0.02	135/1200	9.7 ± 1.1	15.8 ± 1.8
FZ47	7.3 ± 0.3	89/1200	24.9 ± 2.3	0.99 ± 0.01	164/1200	7.7 ± 0.7	23.7 ± 2.4
FZ84	6.0 ± 0.1	171/1200	26.5 ± 1.6	1.00 ± 0.01	242/1200	7.5 ± 0.7	25.4 ± 1.8
FZ85	8.6 ± 0.1	262/1200	21.0 ± 1.1	0.96 ± 0.01	276/1200	6.3 ± 0.6	20.0 ± 1.2
FZ95	4.5 ± 0.1	242/1100	28.2 ± 1.5	0.98 ± 0.01	281/1200	7.9 ± 0.7	27.1 ± 1.6
FZ96	6.0 ± 0.1	176/1200	24.5 ± 1.5	0.99 ± 0.01	195/1200	6.3 ± 0.8	23.7 ± 1.7

437

438

439

440 **E. Equivalent doses for uncrushed and crushed quartz separates**

441

442

Table S7: Sample description and equivalent doses for uncrushed and crushed fractions of zero-age quartzes.

Sample	Provenance	Equivalent dose (Gy)		Increase (Gy) (crushed-uncrushed)
		Uncrushed	Crushed	
BA5	Coastal dune (Armitage et al., 2006)	0.04 ± 0.01	0.23 ± 0.02	0.19 ± 0.02
CH62	Shoreline (Armitage et al., 2015)	0.01 ± 0.01	0.11 ± 0.02	0.10 ± 0.02
FZ16	Desert dune (Armitage et al., 2007)	0.04 ± 0.03	0.12 ± 0.04	0.08 ± 0.05
FZ32	Desert dune (Armitage and Bailey, 2005a)	0.08 ± 0.08	0.16 ± 0.08	0.08 ± 0.12
IN22	Coastal dune (Armitage et al., 2006)	0.01 ± 0.02	0.02 ± 0.01	0.01 ± 0.02
Risø quartz	Calibration sample (Hansen et al., 2015)	0.00 ± 0.00	0.09 ± 0.01	0.09 ± 0.01
SA10	Coastal dune (this study)	0.00 ± 0.00	0.93 ± 0.33	0.93 ± 0.33
			Mean	0.21 ± 0.12

443

444

Table S8: Sample description and equivalent doses for uncrushed and crushed fractions of Holocene quartzes.

Sample	Provenance	Equivalent dose (Gy)		Ratio (uncrushed/crushed)
		Uncrushed	Crushed	
CH22	Shoreline (Armitage et al., 2015)	3.72 ± 0.13	4.07 ± 0.19	1.09 ± 0.06
IN15	Coastal dune (Armitage et al., 2006)	5.35 ± 0.07	5.31 ± 0.06	0.99 ± 0.02
IN16	Coastal dune (Armitage et al., 2006)	2.34 ± 0.11	2.53 ± 0.12	1.08 ± 0.07
NG38	Shoreline (Armitage et al., 2015)	19.5 ± 0.2	20.3 ± 1.2	1.04 ± 0.06
NG39	Shoreline (Armitage et al., 2015)	19.1 ± 0.8	19.4 ± 0.5	1.02 ± 0.05
			Mean	1.04 ± 0.02

445

446

447

448

References

449

450

451

452

453

454

455

456

457

458

459

460

461

462

463

464

465

466

467

468

469

470

471

472

473

474

475

476

Aitken, M.J., 1985. Thermoluminescence dating. Academic press.

Armitage, S., Bailey, R., 2005a. The measured dependence of laboratory beta dose rates on sample grain size. *Radiat Meas* 39, 123-127.

Armitage, S., Duller, G., Wintle, A., 2000. Quartz from southern Africa: sensitivity changes as a result of thermal pretreatment. *Radiat Meas* 32, 571-577.

Armitage, S.J., Bailey, R.M., 2005b. The measured dependence of laboratory beta dose rates on sample grain size. *Radiat Meas* 39, 123-127.

Armitage, S.J., Botha, G.A., Duller, G.A.T., Wintle, A.G., Rebelo, L.P., Momade, F.J., 2006. The formation and evolution of the barrier islands of Inhaca and Bazaruto, Mozambique. *Geomorphology* 82, 295-308.

Armitage, S.J., Bristow, C.S., Drake, N.A., 2015. West African monsoon dynamics inferred from abrupt fluctuations of Lake Mega-Chad. *P Natl Acad Sci USA* 112, 8543-8548.

Armitage, S.J., Drake, N.A., Stokes, S., El-Hawat, A., Salem, M., White, K., Turner, P., McLaren, S.J., 2007. Multiple phases of north African humidity recorded in lacustrine sediments from the fazzan basin, Libyan sahara. *Quat Geochronol* 2, 181-186.

Armitage, S.J., Jasim, S.A., Marks, A.E., Parker, A.G., Usik, V.I., Uerpmann, H.-P., 2011. The Southern Route "Out of Africa": Evidence for an Early Expansion of Modern Humans into Arabia. *Science* 331, 453-456.

Armitage, S.J., King, G.E., 2013. Optically stimulated luminescence dating of hearths from the Fazzan Basin, Libya: A tool for determining the timing and pattern of Holocene occupation of the Sahara. *Quat Geochronol* 15, 88-97.

Bailey, R.M., Armitage, S.J., Stokes, S., 2005. An investigation of pulsed-irradiation regeneration of quartz OSL and its implications for the precision and accuracy of optical dating (Paper II). *Radiat Meas* 39, 347-359.

Ballarini, M., Wintle, A.G., Wallinga, J., 2006. Spatial variation of dose rate from beta sources as measured using single grains. *Ancient TL* 24, 1-7.

Bateman, M.D., Swift, D.A., Piotrowski, J.A., Sanderson, D.C.W., 2012. Investigating the effects of glacial shearing of sediment on luminescence. *Quat Geochronol* 10, 230-236.

477 Bøtter-Jensen, L., Andersen, C.E., Duller, G.A.T., Murray, A.S., 2003. Developments in radiation,
478 stimulation and observation facilities in luminescence measurements. *Radiat Meas* 37, 535-541.
479 Brennan, B.J., 2003. Beta doses to spherical grains. *Radiat Meas* 37, 299-303.
480 Brennan, B.J., Lyons, R.G., Phillips, S.W., 1991. Attenuation of alpha particle track dose for
481 spherical grains. *International Journal of Radiation Applications and Instrumentation. Part 18*, 249-
482 253.
483 Cunningham, A.C., Devries, D.J., Schaart, D.R., 2012. Experimental and computational simulation
484 of beta-dose heterogeneity in sediment. *Radiat Meas* 47, 1060-1067.
485 Duller, G., 2007. Assessing the error on equivalent dose estimates derived from single aliquot
486 regenerative dose measurements. *Ancient TL* 25, 15-24.
487 Duller, G.A.T., 2003. Distinguishing quartz and feldspar in single grain luminescence
488 measurements. *Radiat Meas* 37, 161-165.
489 Duller, G.A.T., Bøtter-Jensen, L., Murray, A.S., Truscott, A.J., 1999. Single grain laser
490 luminescence (SGLL) measurements using a novel automated reader. *Nuclear Instruments and*
491 *Methods in Physics Research, Section B: Beam Interactions with Materials and Atoms* 155, 506-
492 514.
493 Galbraith, R.F., Roberts, R.G., Laslett, G.M., Yoshida, H., Olley, J.M., 1999. Optical dating of
494 single and multiple grains of quartz from Jinmium rock shelter, northern Australia: Part I,
495 experimental design and statistical models. *Archaeometry* 41, 339-364.
496 Guérin, G., Jain, M., J. Thomsen, K., S. Murray, A., Mercier, N., 2015. Modelling dose rate to
497 single grains of quartz in well-sorted sand samples: The dispersion arising from the presence of
498 potassium feldspars and implications for single grain OSL dating. *Quat Geochronol* 27, 52-65.
499 Guérin, G., Mercier, N., 2012. Preliminary insight into dose deposition processes in sedimentary
500 media on a scale of single grains: Monte Carlo modelling of the effect of water on the gamma dose
501 rate. *Radiat Meas* 47, 541-547.
502 Hansen, V., Murray, A., Buylaert, J.P., Yeo, E.Y., Thomsen, K., 2015. A new irradiated quartz for
503 beta source calibration. *Radiat Meas* 81, 123-127.
504 Martin, L., Mercier, N., Incerti, S., Lefrais, Y., Pecheyran, C., Guérin, G., Jarry, M., Bruxelles, L.,
505 Bon, F., Pallier, C., 2015. Dosimetric study of sediments at the beta dose rate scale:
506 Characterization and modelization with the DosiVox software. *Radiat Meas* 81, 134-141.
507 Mayya, Y.S., Morthekai, P., Murari, M.K., Singhvi, A.K., 2006. Towards quantifying beta
508 microdosimetric effects in single-grain quartz dose distribution. *Radiat Meas* 41, 1032-1039.
509 Murray, A.S., Wintle, A.G., 2000. Luminescence dating of quartz using an improved single-aliquot
510 regenerative-dose protocol. *Radiat Meas* 32, 57-73.
511 Rhodes, E.J., Fanning, P.C., Holdaway, S.J., 2010. Developments in optically stimulated
512 luminescence age control for geoarchaeological sediments and hearths in western New South
513 Wales, Australia. *Quat Geochronol* 5, 348-352.
514 Rhodes, E.J., Fanning, P.C., Holdaway, S.J., Bolton, C.C., 2009. Archaeological surfaces in western
515 NSW: stratigraphic contexts and preliminary OSL dating of hearths. *Terra Australis* 28, 12.
516 Swift, D.A., Sanderson, D.C.W., Nienow, P.W., Bingham, R.G., Cochrane, I.C., 2011. Anomalous
517 luminescence of subglacial sediment at Haut Glacier d'Arolla, Switzerland - a consequence of
518 resetting at the glacier bed? *Boreas* 40, 446-458.
519 Thomsen, K.J., Murray, A.S., Bøtter-Jensen, L., 2005. Sources of variability in OSL dose
520 measurements using single grains of quartz. *Radiat Meas* 39, 47-61.
521 Thomsen, K.J., Murray, A.S., Buylaert, J.P., Jain, M., Hansen, J.H., Aubry, T., 2016. Testing
522 single-grain quartz OSL methods using sediment samples with independent age control from the
523 Bordes-Fitte rockshelter (Roches d'Abilly site, Central France). *Quat Geochronol* 31, 77-96.
524
525